



Preparation, Characterization and Molecular Docking Study of some New Pyrazole Derivatives Derived from 2-Mercaptobenzothiazole

Jassim A. Jassim

Nineveh Education Directorate/ Iraqi Ministry of Education

Salim J. Mohammed

Chemistry Department/ College of Science/ University of Mosul/ Mosul

Zeyad A. Hameed

Department of Chemistry Sciences/ School of Natural and Applied Sciences/ Çankırı Karatekin University/ Turkey

p-ISSN: 1608-9391
e-ISSN: 2664-2786

Article information

Received: 28/12/2024

Revised: 21/2/2025

Accepted: 2/3/2025

DOI:
[10.33899/rjs.2025.187743](https://doi.org/10.33899/rjs.2025.187743)

corresponding author:
Jassim A. Jassim
aljoporyjassim@gmail.com

ABSTRACT

In this research, a series of pyrazole derivatives were prepared through a series of reactions starting from the reaction of the starting material mercaptobenzothiazole with ethyl cyanoacetate to prepare the thioester compound (1) and then reacting it with some benzaldehyde derivatives to prepare the α , β -unsaturated carbonyl compounds (2a-h) after which hydrazine is added to obtain the pyrazole derivatives. (3a-h). The prepared compounds were identified and confirmed by FT-IR and ¹H-NMR spectroscopy. A comparative study was also conducted between finasteride, 5- α reductase inhibitor, and pyrazole derivatives through a computational comparative survey using molecular docking. Androgenetic alopecia (AGA) continues to be widespread skin issue caused by hormones, mainly due to dihydrotestosterone. The purpose of the current study was to prepare and evaluate the pyrazole derivatives as the 5 α -reductase inhibitors responsible for DHT synthesis. Molecular docking uses the crystal structure of steroid 5 α -reductase (PDB: 7BW1) to show that compounds 3a, 3c and 3b exhibit good MolDock and Rerank scores as well as strong hydrogen bonding with the active site of the enzyme. Among these, compound 3a has the highest binding affinity (MolDock Score of -172.891). The docking studies revealed crucial interactions between the docked molecules and the targeted enzyme amino acids, including conventional hydrogen bonds, π -stacking, and van der Waals forces, all of which stabilize the ligand-enzyme complex. The pyrazole derivatives can be used as a drug in AGA treatment as per results. Although, more laboratory and animal tests are needed to prove the effect and safety in humans of these medicines.

Keywords: Pyrazole, mercapto benzothiazole, thioester, finasteride, molecular ducing

INTRODUCTION

Pyrazoles are important heterocyclic compounds due to their wide and intensive use in various fields, especially in medicinal and pharmaceutical chemistry (Kotnala *et al.*, 2024). Also, pyrazole derivatives have different biological activity (Gwady *et al.*, 2010) such as anticancer (Wang *et al.*, 2020) antimicrobial (Desai *et al.*, 2020) antiviral (Yang *et al.*, 2021) antagonist (Harcken *et al.*, 2019) analgesic (Aggarwal *et al.*, 2020) anti-inflammatory (Nayak *et al.*, 2020) antioxidant (Vagish *et al.*, 2021) anthelmintic (Bhavsar *et al.*, 2020) herbicidal (Shawkat and Omar, 2012) (Fu *et al.*, 2020) and antimitotic activities (Zhang *et al.*, 2020), Pyrazole was first prepared by the scientist Ludwig Knorr 1883 (Alam *et al.*, 2015), Then many methods were developed to prepare pyrazole, one of these methods is the reaction of α,β -unsaturated carbonyl compounds with hydrazine hydrate. The thioester compound containing the active methylene group was relied upon to prepare α,β -unsaturated carbonyl compounds by reacting with aldehyde substituents (Al-Saheb *et al.*, 2020). A lot of people have androgenic alopecia (AGA), which is a kind of male pattern baldness. (Koch *et al.*, 2020). The factors that lead to AGA include an imbalance in androgen hormones, stress, genetic illnesses, starvation, an overactive 5α -reductase type II ($5\alpha R2$), malfunction in the thyroid gland, addiction to drugs, and aging (Richards *et al.*, 2008). Most androgens, including testosterone, are primarily produced by the testicles and converted to dihydrotestosterone (DHT) via $5\alpha R2$, pharmacological treatments using synthetic medications like finasteride or minoxidil, and hair follicle regeneration utilizing altered stem cells (Gupta *et al.*, 2017). Androgenetic alopecia is treated by finasteride, which is an oral selective 5-alpha-reductase inhibitor (Mysore and Shashikumar, 2016). Severe dermatological adverse effects, such as decreased libido, irritation, itching, erythema, and depression, have been recorded with these medications (Yim *et al.*, 2014). Therefore, it is critical to find a new pharmacological drug that promotes hair growth without causing any side effects. One possible method for developing future pharmaceutical treatments to treat a variety of diseases is computer-aided drug design (CADD), which has just come into its own (Llorach-Pares *et al.*, 2022). In this case, we want to use a computational technique to discover new chemical compounds that might be used as $5\alpha R2$ inhibitors cure AGA.

MATERIALS AND METHODS

Compounds that were used in this study: All compounds were obtained from Aldrich, BDH, and Fluka companies. The melting point apparatus was recorded by Stuart (SPM30). Compounds determined and characterized by spectroscopy methods 1H -NMR was recorded by DMSO- d_6 at 400 MHz with TMS as the internal standards and Infrared (FT-IR) spectra were recorded using ATR-FTIR Spectrophotometer. The thin-layer chromatography (TLC) was carried out on an Eastman chromatogram sheet (20x20) cm, 13181 silica gel with the fluorescent indicator (No. 6060) with solvent system benzene: Methanol with a ratio of (8:2).

EXPERIMENTAL

Synthesis of (1,3-benzothiazol-2-yl) cyanoethanethioate (1)

Equal quantities (0.0239 mol) of 2-mercapto-benzothiazole were mixed with K_2CO_3 in dry acetone in a (250 ml) conical flask equipped with a magnetic stirrer for 30 min at laboratory temperature, followed by the gradually addition of (3.5 ml) of ethyl cyanoacetate. After the completion of the addition, the mixture was refluxed for (5 hours) and the reaction was monitored by TLC. After the reaction was completed, the mixture was cooled and filtered to get rid of the reaction residues. Then, the filtrate was placed under vacuum to get rid of the solvent and obtain the product, and it was recrystallized using ethanol absolute. ATR-FTIR: $C\equiv N$ (2184); $C=O$ (1660); $C=N$ (1596); $C-S$ (749) cm^{-1} . 1H -NMR (400 MHz, DMSO) (ppm) 7.39 (d, $J = 7.6$ Hz, 1H), 7.25 (d, $J = 7.9$ Hz, 1H), 7.07 (s, 1H), 6.92 (d, $J = 7.5$ Hz, 1H), 3.97 (s, 2H).

Synthesis of α,β -unsaturated carbonyl (2a-h) (Abu-Hashem and Gouda, 2017)

These compounds are prepared by mixing equivalent moles (0.00427 mol) of 1 and substituted benzaldehyde in (20 ml) of absolute ethanol and (0.5 ml) of piperidine. The mixture is

then heated for (5 hours) and the reaction is monitored by TLC. After then the reaction is complete, the mixture is cooled and poured into crushed ice to precipitate. Then filtered to obtain the resulting product and recrystallized using absolute ethanol. The physical and spectral data were listed in the (Table 1,3 and 5).

Synthesis of pyrazole derivatives(3a-h) (Bondock *et al.*, 2010).

The pyrazole compounds are prepared by dissolving (0.00224 mol) of the compounds 2a-h in (20 ml) of absolute ethanol, then (0.00898 mol) of aqueous hydrazine is added gradually, then the mixture is heated for (3 hours) and the reaction is monitored by TLC. After the reaction is complete, the mixture is cooled and poured into crushed ice to precipitate, then it is filtered to obtain the resulting product, which is recrystallized using absolute ethanol. The physical and spectral data were listed in (Table 2,4 and 6).

Table 1: The physical properties of compounds (2a-h)

Comp.	-R	M.P(°C)	Yield%	Colour
2a	3-NO ₂ -C ₆ H ₄	200-202	68	Yellow
2b	2-OH-3-OCH ₃ -C ₆ H ₃	255-257	66	Brown
2c	3,4-OCH ₂ O-C ₆ H ₃	230-232	65	Brown
2d	4-N(CH ₃) ₂ -C ₆ H ₄	217-220	70	Brown
2e	4-Br-C ₆ H ₄	256-259	65	Brown
2f	3-CH ₃ -C ₆ H ₄	190-192	60	Light Brown
2g	4-Cl-C ₆ H ₄	219-221	80	Orange
2h	2,4-diCl-C ₆ H ₃	258-260	70	Yellow

Table 2: Physical properties of compounds (3a-h)

Comp.	-R	M.P(°C)	Yield%	Colour
3a	3-NO ₂ -C ₆ H ₄	234-236	58	Yellow
3b	2-OH-3-OCH ₃ -C ₆ H ₃	277-279	50	Yellow
3c	3,4-OCH ₂ O-C ₆ H ₃	260-262	45	Red
3d	4-N(CH ₃) ₂ -C ₆ H ₄	250-252	60	Light Brown
3e	4-Br-C ₆ H ₄	230-232	65	Red
3f	3-CH ₃ -C ₆ H ₄	262-265	70	Light Brown
3g	4-Cl-C ₆ H ₄	238-240	75	Red
3h	2,4-diCl-C ₆ H ₃	230-232	52	Dark Brown

Table 3: Data of FT-IR of compounds (2a-h)

Comp.	ATR-FTIR) $\nu(\text{cm}^{-1})$					
	R	C≡N	C=O	C=N	C-S	Others
2a	3-NO ₂ -C ₆ H ₄	2188	1632	1614	757	NO ₂ asym1529 sym1349
2b	2-OH-3OCH ₃ -C ₆ H ₃	2194	1620	1596	753	O-H 3332 CH ₃ asym 2965 Sym2927
2c	3,4-OCH ₂ O-C ₆ H ₃	2185	1661	1622	748	C-H asym 2980 Sym2963
2d	4-N(CH ₃) ₂ -C ₆ H ₄	2185	1660	1600	748	C-H asym 2981 Sym2964
2e	4-Br-C ₆ H ₄	2190	1674	1624	748	C-Br 809
2f	3-CH ₃ -C ₆ H ₄	2190	1674	1602	747	C-H asym 2984 Sym2938
2g	4-Cl-C ₆ H ₄	2183	1660	1623	748	C-Cl 820
2h	2,4-diCl-C ₆ H ₃	2185	1661	1614	748	C-Cl 810

Table 4: Data of FT-IR of compounds (3a-h)

Comp.	ATR-FTIR $\nu(\text{cm}^{-1})$						Others
	-R	NH ₂	NH	C=O	C=N	C-S	
3a	3-NO ₂ -C ₆ H ₄	3317 3280	3199	1646	1597	752	NO ₂ asym 1556 Sym 1344
3b	2-OH-3OCH ₃ -C ₆ H ₃	3240 3208	3150	1620	1596	754	O-H 3333 C-H asym 2967 Sym 2925
3c	3,4-OCH ₂ O-C ₆ H ₃	3377 3326	3206	1660	1602	754	C-H asym 2961 Sym 2925
3d	4-N(CH ₃) ₂ -C ₆ H ₄	3396 3338	3240	1660	1599	743	C-H asym 2953 Sym 2909
3e	4-Br-C ₆ H ₄	3322 3315	3260	1658	1584	756	C-Br 818
3f	3-CH ₃ -C ₆ H ₄	3357 3318	3199	1660	1597	753	C-H asym 2962 Sym 2930
3g	4-Cl-C ₆ H ₄	3357 3317	3199	1649	1596	752	C-Cl 883
3h	2,4-diCl-C ₆ H ₃	3335 3280	3217	1640	1596	754	C-Cl 867

Table 5: Data of ¹H-NMR of compounds (2a-h)

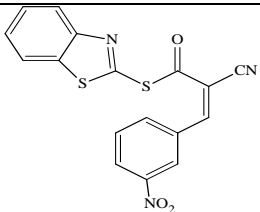
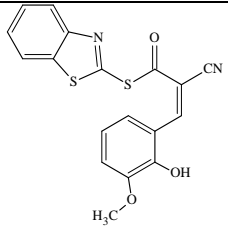
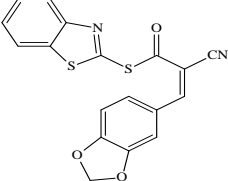
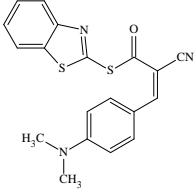
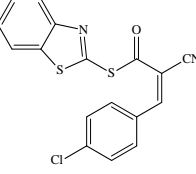
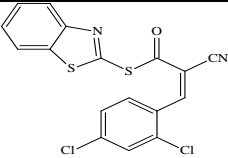
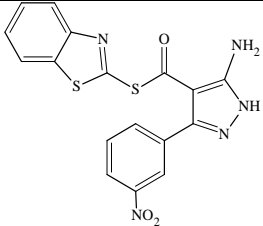
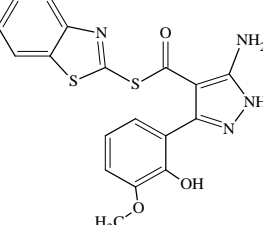
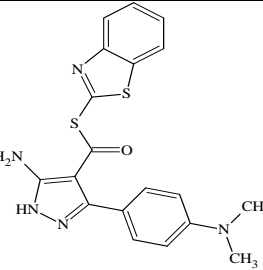
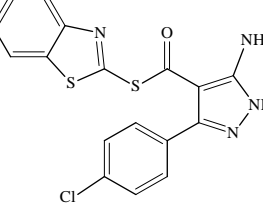
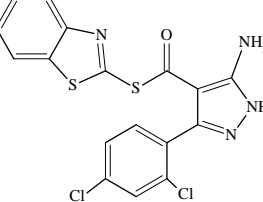
Comp.	Structure	¹ H-NMR (400 MHz, DMSO)
2a		Ar= 8.73 (d, <i>J</i> = 28.9 Hz, 0H), 8.21 (d, <i>J</i> = 21.0 Hz, 1H), 8.07 (d, <i>J</i> = 32.2 Hz, 2H), 7.69 (d, <i>J</i> = 7.9 Hz, 2H), 7.39 (t, <i>J</i> = 7.7 Hz, 2H), 7.34 -7.29 (m, 3H), 7.27 (d, <i>J</i> = 7.8 Hz, 1H), 6.54 (s, 1H), 4.64 (s, 1H. C-CH=C).
2b		9.35 (s, 1H.OH), 8.13 (d, <i>J</i> = 8.0 Hz, 1H), 8.03 (d, <i>J</i> = 8.2 Hz, 1H), 7.54 (t, <i>J</i> = 7.8 Hz, 1H), 7.42 (t, <i>J</i> = 7.8 Hz, 1H), 4.49 (s, 1H. C-CH=C), 3.57 (s, 1H.CH ₃).
2c		7.38 (d, <i>J</i> = 7.7 Hz, 1H), 7.25 (d, <i>J</i> = 7.8 Hz, 1H), 7.10 - 7.03 (m, 1H), 6.90 (t, <i>J</i> = 7.4 Hz, 1H), 3.96 (s, 1H. C-CH=C), 3.69 (s, 2H.CH ₂).
2d		7.38 (s, 4H), 7.24 (s, 1H), 6.91 (s, 2H), 3.96 (s, 1H. C-CH=C), 1.13 (s, 6H.2CH ₃).
2g		7.99 - 7.53 (m, 1H), 7.38 (d, <i>J</i> = 7.6 Hz, 2H), 7.23 (d, <i>J</i> = 7.9 Hz, 2H), 7.06 (t, <i>J</i> = 7.6 Hz, 2H), 6.89 (t, <i>J</i> = 7.4 Hz, 2H), 3.68 (s, 1H. C-CH=C).
2h		7.38 (d, <i>J</i> = 7.7 Hz, 2H), 7.24 (d, <i>J</i> = 7.9 Hz, 2H), 7.07 (t, <i>J</i> = 7.6 Hz, 2H), 6.90 (t, <i>J</i> = 7.4 Hz, 2H), 3.96 (s, 1H. C-CH=C).

Table 6: Data of ¹H-NMR of compounds (3a-h)

Comp.	Structure	¹ H-NMR (400 MHz, DMSO)
3a		8.97 (s, 1H.NH), 7.69-7.64 (m, 3H), 7.32 (d, 2H), 7.20 (s, 3H), 6.97 (d, 2H), 6.52 (s, 2H.NH ₂).
3b		10.68 (s, 1H.NH), 9.35 (s, 1H), 8.11 (d, <i>J</i> = 7.9 Hz, 1H), 8.02 (d, <i>J</i> = 8.2 Hz, 1H), 7.52 (t, <i>J</i> = 7.8 Hz, 1H), 7.41 (t, <i>J</i> = 7.8 Hz, 1H), 6.71 (s, 2H.NH ₂), 3.16 (s, 3H.CH ₃).
3d		9.37 (s, 1H.NH), 8.50 (s, 1H), 7.65 (d, <i>J</i> = 8.5 Hz, 3H), 7.37 (d, <i>J</i> = 7.2 Hz, 1H), 6.77 (s, 2H.NH ₂), 1.24 (s, 6H.2CH ₃).
3g		9.81 (s, 1H.NH), 7.38 (t, <i>J</i> = 5.5 Hz, 1H), 7.25 (d, <i>J</i> = 7.9 Hz, 1H), 7.21 (s, 3H), 7.06 (q, <i>J</i> = 5.7 Hz, 1H), 6.87 (s, 2H.NH ₂).
3h		9.79 (s, 1H.NH), 7.38 (d, <i>J</i> = 8.2 Hz, 1H), 7.24 (d, <i>J</i> = 8.0 Hz, 1H), 7.06 (t, <i>J</i> = 7.7 Hz, 1H), 6.88 (s, 2H.NH ₂).

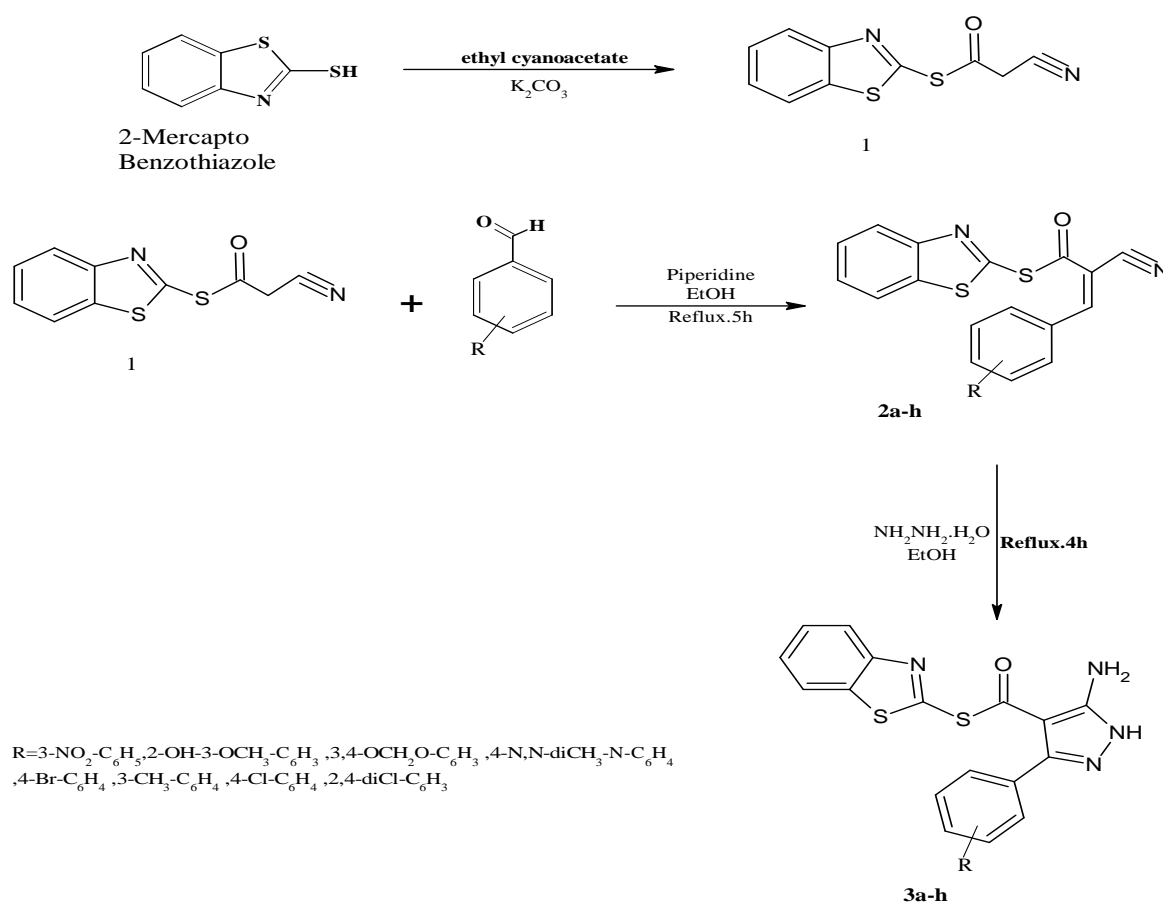
Molecular docking study

The docking process was carried out using a protein data bank structure, namely the 2.80 Å resolution crystal structure of steroid 5-alpha-reductase 2 in association with finasteride (PDB: 7BW1). The PDB ID 7BW1 was allocated to it by (Xiao *et al.*, 2020). Molegro virtual docker was used specifically for the docking experiments. Source: (Thomsen and Christensen, 2006). Protein structures were imported using the software's File/Import molecule's function. Removed water molecules have been from the protein crystal structure. Things that weren't needed for the procedure were taken out. Docking experiments were used for compounds obtained from pyrazole derivatives. The 3D SDF structures of 8 compounds were obtained after being drawn by the ChemDraw program, and their structures were converted to 3D SDF by the Avogadro program. They were received by the docking software. We checked the molecular structures for any errors and corrected them. After fixing the faults, the structure was optimized. The appropriate space was chosen to serve as the compounds' docking point. The docking wizard was launched to initiate the docking procedure. Our team chose the Ligands in the workspace. A scoring function called MolDock score was created. We checked the origin, radius, and center of the binding site. Our search strategy was MolDock SE. A grand total of ten runs were recorded. Following docking, the

objective of minimizing energy and optimizing the H-bond was selected. The docking operation may commence once the destination folder for the results file is determined. The data was fed into the algorithm after docking, and the most promising results were selected for further investigation. When exporting the protein structure and poses, the PDB file was used. You will find these files in the discovery studio 2021 client. This program explained the intricate interactions between chemicals and proteins, along with their binding states.

RESULTS AND DISCUSSION

In this study, synthesis of α , β -unsaturated carbonyl through reaction between thioester and benzaldehyde derivatives by using piperidine as base, the authenticity of the prepared compounds was confirmed by spectroscopic methods (FT-IR and $^1\text{H-NMR}$), where the FT-IR showed the disappearance of the distinctive aldehyde band as we see in (Table 3), while in the nuclear magnetic resonance spectrum, the authenticity of the formation of the compounds was confirmed by the disappearance of the aldehyde signals as well as the disappearance of the active methylene signals in addition to the appearance of the $\text{HC}=\text{C}$ signals as we see in (Table 5). Then, these compounds were introduced into the reaction with hydrazine hydrate to prepare pyrazole derivatives as in scheme (1), which were also identified through the infrared spectrum, where the primary and secondary amine band appeared at (3396-3240) (3338-3240) and (3240-3150) cm^{-1} respectively and the nitrile band disappeared as we see in (Table 4). In $^1\text{H-NMR}$, the primary and secondary amine signals also appeared in addition to the disappearance of the $\text{HC}=\text{C}$ signal in addition to other distinctive signals as we see in (Table 6), which provided evidence of the authenticity of the formation of the prepared compounds. And then we used pyrazole derivatives to compare them with finasteride.



Scheme 1: Equation of synthesis of pyrazole derivatives.

Molecular docking

(Table 7) displays the outcomes of the molecular docking research. The compounds, their PubChem CIDs, MolDock scores, Rerank scores, and HBonds are all shown accordingly.

Table 7: Experiment findings from molecular docking

Ligand	MolDock Score	Rerank Score	HBond
3a	-172.891	-71.3832	-11.2498
3c	-172.551	-93.5301	-10.7938
3b	-172.113	-69.6875	-14.6109
3f	-158.248	-95.0003	-8.94175
3h	-157.203	-108.421	-4.76622
3d	-155.622	-110.142	-2.49417
3g	-153.057	-104.179	-3.09215
3e	-150.533	-113.358	-3.28969

The MolDock scoring function determines the total binding energy of the ligand to the target, which is represented by the MolDock score. Better binding affinity is often indicated by lower MolDock scores. To further improve the ranking of the ligands, this score is likely employed as a supplementary scoring method. Unlike the MolDock score, it may use a distinct set of chemical and physical characteristics. This value stands for the total number of hydrogen bonds established between the ligand and the target. The stability of molecular interactions and bonding relies on hydrogen bonds.

The results of the molecular docking investigation conducted using Molegro virtual docker are shown in (Table 1). In this investigation, the target protein was alpha-5 reductase, and the purpose of this software was to predict the binding affinity of ligands to the protein. (Table 1) displays the binding affinities of several substances to alpha 5 reductase. The better ligand that shows the greatest promise is 3a, which has a Moledoc score of -172.891, and a rearrangement score of -71.3832. Along with the enzyme, it creates a hydrogen bond. 3c the Moledoc201 score of -172.551, and rearrangement score of -93.5301 of these molecules are comparable to those of 3a, indicating that it might potentially be a powerful ligand as well. 3b demonstrates a strong binding affinity, although having a lower Moledoc score of -172.113, compared to 3c and 3a.

Interactions between proteins and ligands rely heavily on hydrogen bonding. A higher affinity is often seen for compounds that have a larger number of hydrogen bonds.

Both the MolDock score and the Rerank score place ligand 3a at the top of the list of ligands. It also contains more hydrogen bonds than any other compound, which means it interacts strongly with its target. The ligands 3b, 3c, and 3f also have high binding affinity, as shown by their favorable MolDock and Rerank scores. A large number of hydrogen bonds are also present in them. Weak binding relative to the top-ranking ligands is suggested by the lower MolDock and Rerank scores of ligands 3d, 3e, 3g, and 3h. Additionally, their hydrogen bond count is lower. According to the (Table 1), ligand 3a has the best combination of hydrogen bonding, MolDock score, and Rerank score, making it the most promising contender.

The compound 3a binds to 5-alpha-reductase through several bonds: Conventional hydrogen bond (TYR A:33, LYS A:35, ASN A:102, ARG A:107, ASP A:164, and ARG A;171), and carbon hydrogen bond (GLY A:104), the stabilization of the ligand-protein complex is greatly aided by these robust electrostatic interactions. The existence of several hydrogen bonds indicates a binding relationship that is favorable. Unfavorable bump (GLY A:34), these destabilize the complex because steric conflicts happen when ligand and protein atoms are too near to one another. Pi-sulfur (TYR A:178), Pi-Pi T-shaped (HIS A:231), Pi-alkyl (ALA A:49, and LEU A:167), aromatic rings that contain pi electrons may engage in Pi-Pi interactions. Van der Waals the weak non-covalent forces known as van der Waals interactions, which originate from transient dipoles, are shown by the light green. Both the ligand's and the protein's binding affinity and form complementarity are

influenced by these interactions. Fig. (1) shows both the 2D and 3D models of the complexes formed.

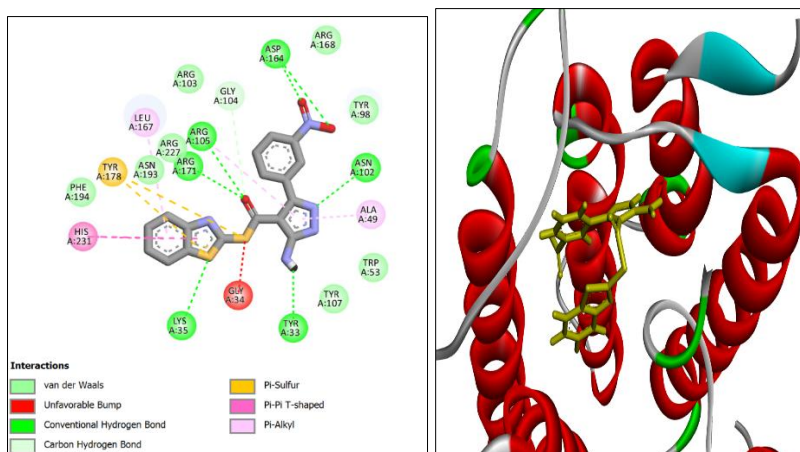


Fig. 1: Interactions between 3a and 5-alpha-reductase.

The compound 3c binds to 5-alpha-reductase through several bonds: Conventional hydrogen bond (TYR A:33, TYR A:98, ASN A:102, ARG A:105, ARG A:171, and TYR A:178), and carbon hydrogen bond (GLY A:104), the stabilization of the ligand-protein complex is greatly aided by these robust electrostatic interactions. The existence of several hydrogen bonds indicates a binding relationship that is favorable. Unfavorable bump (GLY A:34), and unfavorable donor-donor (TRP A:53) destabilize the complex because steric conflicts happen when ligand and protein atoms are too near to one another. Pi-sulfur (TYR A:33, and HIS A:231), Pi-Pi T-shaped (HIS A:231), Pi-alkyl (ALA A:49, and LEU A:167), and alkyl (TYR A:98, and LEU A:167) aromatic rings that contain Pi electrons may engage in Pi-Pi interactions. Van der Waals the weak non-covalent forces known as van der Waals interactions, which originate from transient dipoles, are shown by the light green. Both the ligand's and the protein's binding affinity and form complementarity are influenced by these interactions. Fig. (2) shows both the 2D and 3D models of the complexes formed.

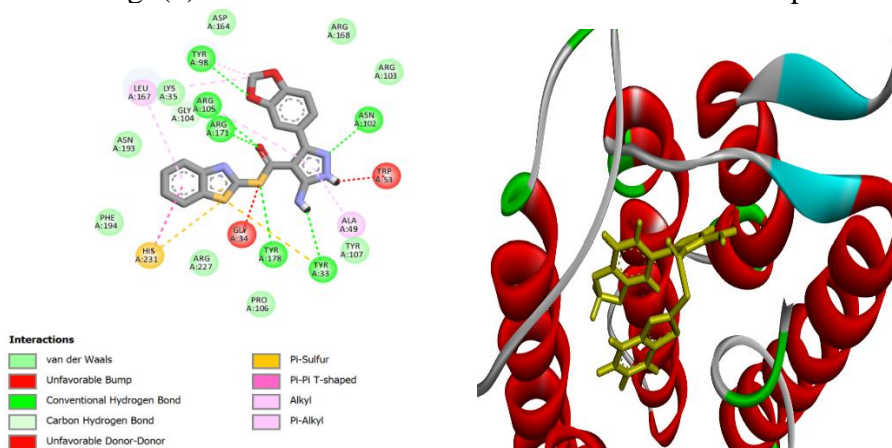


Fig. 2: Interactions between 3c and 5-alpha-reductase.

The compound 3b binds to 5-alpha-reductase through several bonds: Conventional hydrogen bond (TYR A:33, LYS A:35, ASN A:102, ARG A:105, and ARG A:171), and carbon hydrogen bond (ASP A:164), the stabilization of the ligand-protein complex is greatly aided by these robust electrostatic interactions. The existence of several hydrogen bonds indicates a binding relationship that is favorable. Unfavorable bump (GLY A:34), and unfavorable donor-donor (TRP A:53), destabilize the complex because steric conflicts happen when ligand and protein atoms are too near to one another. Pi-sulfur (TYR A:178), Pi-Pi T-shaped (HIS A:231), Pi-alkyl (ALA A:49), and alkyl (TYR A:98, and LEU A:167) aromatic rings that contain Pi electrons may engage in Pi-Pi

interactions. Van der Waals the weak non-covalent forces known as Van der Waals interactions, which originate from transient dipoles, are shown by the light green. Both the ligand's and the protein's binding affinity and form complementarity are influenced by these interactions. Fig. (2) shows both the 2D and 3D models of the complexes formed.

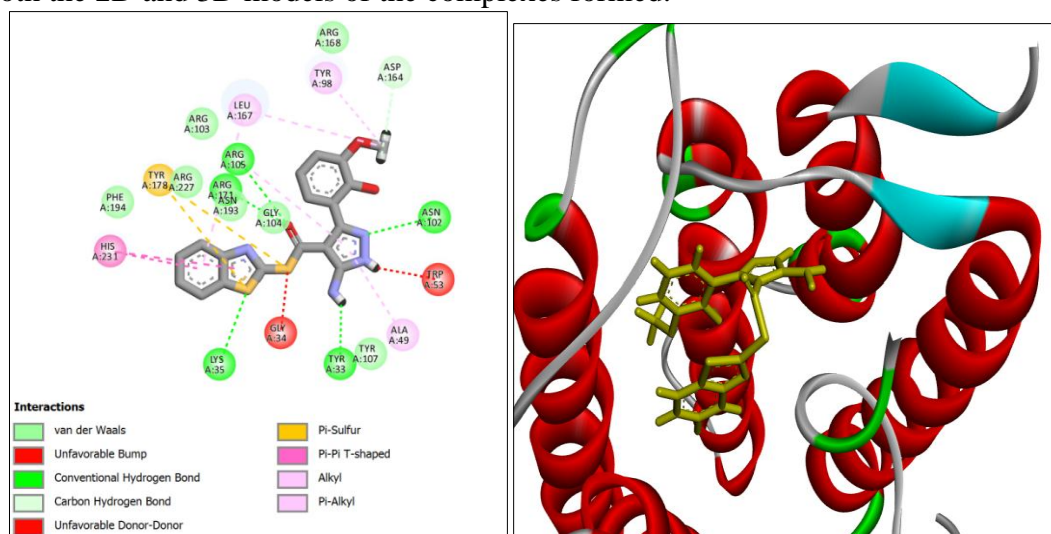


Fig. 3: Interactions between 3b and 5-alpha-reductase.

Multiple hydrogen bonds and Van der Waals interactions indicate that the ligand and protein are bound in a favorable manner. The complex is even more stable because of the Pi-Pi interactions. Unfortunately, the ligand could need optimization to enhance its protein fit and reduce steric conflicts due to the existence of unfavorable bump interactions. Names of residues: The labels on the protein residues tell you what the amino acid is and where it is in the protein sequence. For example, an arginine residue would be labeled as ARG and its location in the sequence would be A:168. Pocket for binding: A protein's binding pocket is the specific area to which a ligand binds. The image-based interactions shed light on the binding pocket's general structure and characteristics as well as the essential residues engaged in ligand binding.

CONCLUSIONS

Firstly, pyrazole derivatives were prepared from a series reactions as mentioned above. Finally, the possibility of using chemicals derived from pyrazole derivatives as 5 α -reductase inhibitors, an important enzyme in androgenetic alopecia, was investigated in this research. Potential possibilities were found to be 3a, 3c, and 3b using molecular docking. Pyrazole derivatives showed promising activity against AGA due to their high binding affinities to the enzyme. Their potential as therapeutic solutions, however, depends on the results of further *in vitro* and *in vivo* investigations that verify their efficacy and safety.

REFERENCES

- Abu-Hashem, A.; Gouda, M. (2017). Synthesis and antimicrobial activity of some novel quinoline, chromene, pyrazole derivatives bearing triazolopyrimidine moiety. *J. Heter. Chem.*, **54**(2), 850-858. DOI: 10.1002/jhet.2645
- Aggarwal, R.; Kaushik, P.; Kumar, A.; Saini, D. (2020). Design, synthesis and biological evaluation of 5-amino-3-aryl-1-(6'-chloropyridazin-3'-yl) pyrazoles and their derivatives as analgesic agents. *Drug Res.*, **70**(11), 493-502. DOI: 10.1055/a-1202-9959
- Alam, M.J.; Alam, O.; Alam, P.; Naim, M.J. (2015). A review on pyrazole chemical entity and biological activity. *Inter. J. Pharm. Sci. Res.*, **6**, 1433-1442.

- Al-Saheb, R.; Makharza, S.; Al-Battah, F.; Abu-El-Halawa, R.; Kaimari, T.; Abu Abed, O.S. (2020). Synthesis of new pyrazolone and pyrazole-based adamantyl chalcones and antimicrobial activity. *Biosci. Rep.*, **40**(9), BSR20201950. DOI: 10.1042/BSR20201950
- Bhavsar, Z.A.; Acharya, P.T.; Jethava, D.J.; Patel, H.D. (2020). Recent advances in development of anthelmintic agents: Synthesis and biological screening. *Synth. Comm.*, **50**(7), 917-946. DOI: 10.1080/00397911.2019.1695276
- Bondock, S.; Fadaly, W.; Metwally, M.A. (2010). Synthesis and antimicrobial activity of some new thiazole, thiophene and pyrazole derivatives containing benzothiazole moiety. *European J. Med. Chem.*, **45**(9), 3692-3701. DOI: 10.1016/j.ejmech.2010.05.018
- Desai, N.C.; Vaja, D.V.; Jadeja, K.A.; Joshi, S.B.; Khedkar, V.M. (2020). Synthesis, biological evaluation and molecular docking study of pyrazole, pyrazoline clubbed pyridine as potential antimicrobial agents. *Anti-Infect. Age.*, **18**(3), 306-314. DOI: 10.2174/2211352517666190627144315
- Fu, Q.; Cai, P.P.; Cheng, L.; Zhong, L.K.; Tan, C.X.; Shen, Z.H.; Han, L.; Xu, T.M.; Liu, X.H. (2020). Synthesis and herbicidal activity of novel pyrazole aromatic ketone analogs as HPPD inhibitor. *Pest Manag. Sci.*, **76**(3), 868-879. DOI: 10.1002/ps.5591
- Gupta, A.; Carviel, J.; MacLeod, M.; Shear, N. (2017). Assessing finasteride-associated sexual dysfunction using the FAERS database. *J. European Acad. Dermat.Vener.* **31**(6), 1069-1075. DOI: 10.1111/jdv.14223
- Gwady, M.S.A.; Sheet, A.M.; Saied, S.M. (2010). Some important reactions of 4-aminoantipyrine (4-AAP). *Raf. J. Sci.*, **21**(1E).
- Harken, C.; Sarko, C.; Mao, C.; Lord, J.; Raudenbush, B.; Razavi, H.; Liu, P.; Swinamer, A.; Disalvo, D.; Lee, T. (2019). Discovery and optimization of pyrazole amides as antagonists of CCR1. *Bioor. Med. Chem. Lett.*, **29**(3), 435-440. DOI: 10.1016/j.bmcl.2018.11.015
- Koch, S.L.; Tridico, S.R.; Bernard, B.A.; Shriver, M.D.; Jablonski, N.G. (2020). The biology of human hair: A multidisciplinary review. *American J. Human Bio.*, **32**(2), e23316. DOI: 10.1002/ajhb.23316
- Kotnala, M.; Singh, G.; Singh, K.; Nath, R.; Panda, K.C.; Kumar, A.; Dutta, S. (2024). Exploring the synthetic strategies and biological activities of pyrazole derivatives. *Natur. Camp.*, **28**(1), 3238-3248.
- Llorach-Pares, L.; Nonell-Canals, A.; Avila, C.; Sanchez-Martinez, M. (2022). Computer-aided drug design (cadd) to de-orphanize marine molecules: Finding potential therapeutic agents for neurodegenerative and cardiovascular diseases. *Mar. Drugs*, **20**(1), 53. DOI: 10.3390/md20010053
- Mysore, V.; Shashikumar, B. (2016). Guidelines on the use of finasteride in androgenetic alopecia. *Indian J. Dermat., Vener. Lepr.*, **82**, 128. DOI: 10.4103/0378-6323.177432
- Nayak, S.G.; Poojary, B.; Kamat, V. (2020). Novel pyrazole-clubbed thiophene derivatives via Gewald synthesis as antibacterial and anti-inflammatory agents. *Arc. Pharm.*, **353**(12), 2000103. DOI: 10.1002/ardp.202000103
- Richards, J.B.; Yuan, X.; Geller, F.; Waterworth, D.; Bataille, V.; Glass, D.; Song, K.; Waeber, G.; Vollenweider, P.; Aben, K.K. (2008). Male-pattern baldness susceptibility locus at 20p11. *Nat. Gen.*, **40**(11), 1282-1284. DOI: 10.1038/ng.255
- Shawkat, S.S.; Omar, A.O. (2012). Synthesis of some novel pyrazolo and triazolo quinolines from coumarin compounds. *Raf. J. Sci.*, **23**(3), 108-116.
- Thomsen, R.; Christensen, M.H. (2006). MolDock: A new technique for high-accuracy molecular docking. *J. Med. Chem.*, **49**(11), 3315-3321. DOI: 10.1021/jm051197e
- Vagish, C.B.; Dileep Kumar, A.; Kumara, K.; Vivek, H.K.; Renuka, N.; Lokanath, N.K.; Kumar, A.K. (2021). Environmentally benign synthesis of substituted pyrazoles as potent antioxidant agents, characterization and docking studies. *J. Iranian Chem. Soc.*, **18**, 479-493. DOI: 10.1007/s13738-020-02042-6
- Wang, G.; Liu, W.; Peng, Z.; Huang, Y.; Gong, Z.; Li, Y. (2020). Design, synthesis, molecular modeling, and biological evaluation of pyrazole-naphthalene derivatives as potential anticancer

- agents on MCF-7 breast cancer cells by inhibiting tubulin polymerization. *Bioor. Chem.*, **103**, 104141. DOI: 10.1016/j.bioorg.2020.104141
- Xiao, Q.; Wang, L.; Supekar, S.; Shen, T.; Liu, H.; Ye, F.; Huang, J.; Fan, H.; Wei, Z.; Zhang, C. (2020). Structure of human steroid 5 α -reductase 2 with the anti-androgen drug finasteride. *Nat. Comm.*, **11**(1), 5430. DOI: 10.1038/s41467-020-19249-z
- Yang, G.; Zheng, H.; Shao, W.; Liu, L.; Wu, Z. (2021). Study of the *in vivo* antiviral activity against TMV treated with novel 1-(t-butyl)-5-amino-4-pyrazole derivatives containing a 1,3,4-oxadiazole sulfide moiety. *Pest. Biochem. Physio.*, **171**, 104740. DOI: 10.1016/j.pestbp.2020.104740
- Yim, E.; Nole, K.L.B.; Tosti, A. (2014). 5 α -Reductase inhibitors in androgenetic alopecia. *Curr. Opin. Endocrin., Diab. Obes.*, **21**(6), 493-498. DOI: 10.1097/MED.0000000000000112
- Zhang, N.; Huang, M.Z.; Liu, A.P.; Liu, M.H.; Li, L.Z.; Zhou, C.G.; Ren, Y.G.; Ou, X.M.; Long, C.Y.; Sun, J. (2020). Design, synthesis, and insecticidal/acaricidal evaluation of novel pyrimidinamine derivatives containing phenyloxazole moiety. *Chem. Pap.*, **74**, 963-970. DOI: 10.1007/s11696-019-00932-5

تحضير وتشخيص ودراسة الالتحام الجزيئي لبعض مشتقات البيرازول الجديدة المشتقة من 2-مركابتو بنزو ثايازول

جاسم عبد الرزاق جاسم

مديرية تربية نينوى / وزارة التربية

سالم جاسم محمد

قسم الكيمياء / كلية العلوم / جامعة الموصل / الموصل

زياد عادل حميد

قسم الكيمياء / كلية العلوم التطبيقية / جامعة جانكري كاراتيكن / جانكري / تركيا

الملخص

في هذا البحث، تم تحضير سلسلة من مشتقات البيرازول وذلك من خلال سلسلة من التفاعلات التي تبدأ من مفاعلة المادة الأولية مركبتو بنزو ثايازول مع سيانو خلات الاثيل لتحضير مركب ثايو استر (1) ومن ثم تتم مفاعلته مع عدد من مشتقات البنزالددهايد لتحضير مركبات الفا بيتا كاربونيل غير المشبعة (2a-h) وبعد ذلك تتم اضافة الهيدرازين المائي للحصول على مشتقات البيرازول (3a-h). تم تشخيص المركبات المحضرة وتأكيدها من خلال قياس مطيافية FT-IR و¹H-NMR. كذلك تم اجراء دراسة مقارنة بين فيناسترايد مثبت إنزيم 5-ألفا ريدوكتاز ومشتقات البيرازول من خلال دراسة حاسوبية مقارنة باستخدام الالتحام الجزيئي. تظل الثعلبة الأندروجينية (AGA) مشكلة جلدية شائعة جدًا تسببها الهرمونات، ويرجع ذلك أساسًا إلى وجود ثنائي هيدروتستوستيرون. لذلك كان الغرض من الدراسة الحالية هو إعداد وتقييم مشتقات البيرازول كمثبطات لإنزيم 5-ألفا ريدوكتاز المسؤولة عن تخليق DHT. يستخدم الالتحام الجزيئي البنية البلورية لإنزيم 5-ألفا ريدوكتاز الستيرويدي (PDB: 7BW1) لإظهار أن المركبات a3 و c3 و b3 تظهر درجات مولدوك وريرانك جيدة بالإضافة إلى رابطة هيدروجينية قوية مع الموقع النشط للإنزيم. ومن بين هذه المركبات، يتمتع المركب a3 بأعلى درجة ارتباط (درجة مولدوك -172.891). كشفت دراسات الالتحام عن تفاعلات حاسمة بين الجزيئات المرسة والأحماض الأمينية للإنزيم المستهدف بما في ذلك الروابط الهيدروجينية التقليدية، وتكديس π ، وقوى فان دير فالس، وكلها تعمل على تثبيت مركب الربيطة والإنزيم. يمكن استخدام مشتقات البيرازول كدواء في علاج AGA وفقًا للنتائج. على الرغم من أن هناك حاجة إلى المزيد من الاختبارات المعملية والحيوانية لإثبات تأثير وسلامة هذه الأدوية على البشر.

الكلمات الدالة: البيرازول، مركابتو بنزو ثايازول، الالتحام الجزيئي، 5-ألفا ريدوكتاز، فيناسترايد.